Earth and Planetary Science Letters 295 (2010) 329–341

Contents lists available at ScienceDirect

Earth and Planetary Science Letters

journal homepage: www.elsevier.com/locate/epsl

Joint seismic–geodynamic-mineral physical modelling of African geodynamics: A reconciliation of deep-mantle convection with surface geophysical constraints

Alessandro M. Forte [a,*], Sandrine Quéré [b], Robert Moucha [a], Nathan A. Simmons [c], Stephen P. Grand [d], Jerry X. Mitrovica [e], David B. Rowley [f]

[a] GEOTOP, Université du Québec à Montréal, Montréal, Québec, Canada H3C 3P8
[b] Department of Earth Sciences, Utrecht University, 3508 TA Utrecht, The Netherlands
[c] Atmospheric, Earth and Energy Division, Lawrence Livermore National Laboratory, Livermore CA 94551, USA
[d] Jackson School of Geosciences, University of Texas at Austin, Austin TX 78712, USA
[e] Department of Earth and Planetary Sciences, Harvard University, Cambridge MA 02138 , USA
[f] Department of the Geophysical Sciences, The University of Chicago, Chicago IL 60637, USA

ARTICLE INFO

Article history:
Received 28 August 2009
Received in revised form 10 March 2010
Accepted 15 March 2010
Available online 18 May 2010

Editor: R.W. Carlson

Keywords:
seismic tomography
mantle convection
thermochemical buoyancy
geoid and gravity
dynamic topography
superplumes

ABSTRACT

Recent progress in seismic tomography provides the first complete 3-D images of the combined thermal and chemical anomalies that characterise the unique deep-mantle structure below the African continent. We present a tomography-based model of mantle convection that provides an excellent match to fundamental surface geodynamic constraints on internal density heterogeneity that includes both compositional and thermal contributions, where the latter are constrained by mineral physics. The application of this thermochemical convection model to the problem of African mantle dynamics yields a reconciliation of both surface gravity and topography anomalies to deep-seated mantle flow under the African plate, over a wider range of wavelengths than has been possible to date. On the basis of these results, we predict flow in the African asthenosphere characterised by a clear pattern of focussed upwellings below the major centres of late Cenozoic volcanism, including the Kenya domes, Hoggar massif, Cameroon volcanicline, Cape Verde and Canary Islands. The flow predictions also reveal a deep-seated, large-scale, active hot upwelling below the western margin of Africa under the Cape Verde Islands that extends down to the core–mantle boundary. The scale and dynamical intensity of this 'West African Superplume' is comparable to the 'South African Superplume' that has long been assumed to dominate the large-scale flow dynamics in the deep-mantle under Africa. We evaluate the plausibility of the predicted asthenospheric flow patterns through a comparison with seismic azimuthal anisotropy derived from independent analyses of African shear wave splitting data.

1. Introduction

A longstanding problem in African geodynamics is the delineation of the mantle convective flow below the African plate and its relationship to widespread late Cenozoic hotspot volcanic activity, unique basin and swell topography, and ongoing rifting in East Africa (Burke, 1996; Ebinger and Sleep, 1998). A closely related problem is the development of a physical model that can reconcile the multiple surface geophysical manifestations of convection under the African plate, over a wide range of length scales, with the inferences of mantle heterogeneity provided by seismic tomography. Recent improvements in the seismic sampling of 3-D mantle structure under Africa by temporary seismic arrays (e.g. Kaapvaal, Tanzania, and Ethiopia) provide considerable impetus for the development of such a geodynamically consistent convection model. The outstanding challenge we wish to address here is the construction of a convection model that provides optimal fits to a wide suite of geodynamic data that constrain both the mantle density and viscosity structure, and to achieve this reconciliation over the widest possible range of horizontal length scales. We thereby wish to establish the predictive power of this model and explore the implications for flow dynamics below Africa.

Over the past two decades a wide variety of seismic tomography models have consistently revealed long wavelength images of a large low-velocity (and presumably high-temperature) anomaly below southern Africa extending from the core–mantle boundary to the mid mantle. This deep-mantle seismic anomaly has been interpreted as the possible origin of the African 'superswell': the large-scale anomalously high topography that extends from southern African to the Red Sea along the East African Rift Valley (Nyblade and Robinson, 1994). This hypothesis has been supported by independent mantle flow calculations of the origin of African superswell topography using long wavelength global tomography models (Hager et al., 1985; Lithgow-Bertelloni and Silver, 1998; Gurnis et al., 2000). Initial estimates of the time-dependent evolution of the dynamic topography of Africa have

* Corresponding author.
E-mail address: forte60@gmail.com (A.M. Forte).

0012-821X/$ – see front matter © 2010 Elsevier B.V. All rights reserved.
doi:10.1016/j.epsl.2010.03.017

also been modelled using these tomography-based mantle convection models (Gurnis et al., 2000; Conrad and Gurnis, 2003). The most direct expression of the dynamical interaction between the mantle flow under the African continent and associated lithospheric deformation rates has been explored using long wavelength tomography-based mantle flow calculations (Forte et al., 2002; Behn et al., 2004).

To date, tomography-based numerical investigations of mantle convection below Africa have used long wavelength global tomography models (e.g. Ritsema et al., 1999), that resolve structures with scale lengths generally in excess of 1000 km. With this spatial resolution it is difficult to establish a detailed connection between sublithospheric mantle flow patterns and surface manifestations of African hotspot magmatism and related topographic anomalies (e.g. late Cenozoic volcanic domes and massifs) that characterise Africa's unique physiography (Fig. 1). Substantial progress has recently been made in deriving seismic tomography models that approach the horizontal resolution needed to address the modelling challenges outlined above (Priestley et al., 2006; Simmons et al., 2007, 2009; Fishwick et al., 2007).

In this study we focus on the geodynamic implications of a new joint inversion of global seismic and surface geodynamic data sets, in which mineral physical constraints on mantle thermal properties are also included (Simmons et al., 2007, 2009). These tomographic inversions yield 3-D distributions of mantle density anomalies that include both thermal and compositional heterogeneities. We are therefore able to incorporate, for the first time, a complete 3-D mapping of the stabilising effect of chemical buoyancy in the African lower mantle and continental tectosphere. Our first challenge is to verify the geodynamic consistency of these new inferences of mantle buoyancy through direct comparisons with surface geoid, gravity, topography anomalies and surface plate motions.

The subsequent challenge is to employ the inferred density anomalies to elucidate the influence of the buoyancy-driven mantle flow on the motion of the African plate and the implications for

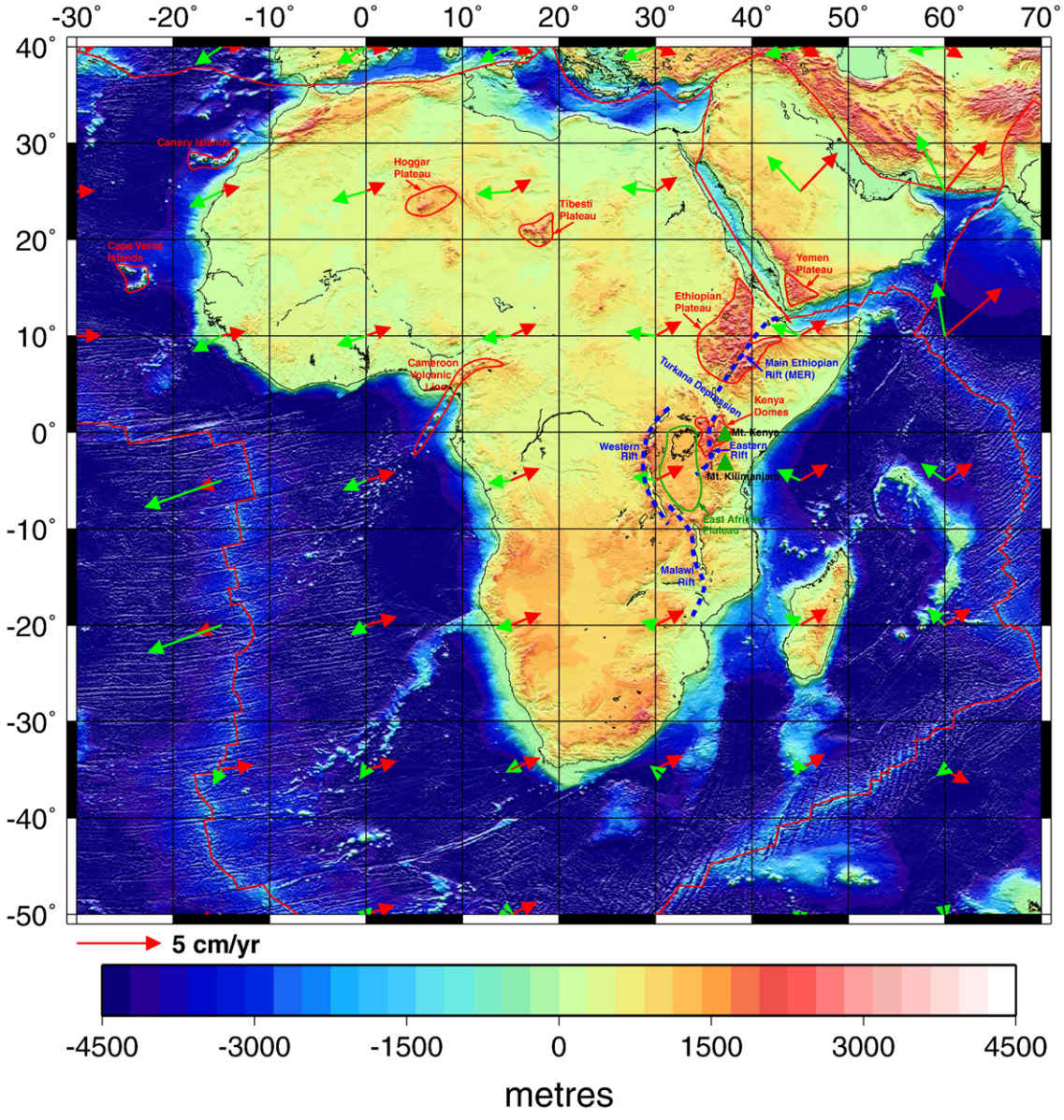

Fig. 1. Topography, bathymetry and velocity of the African plate illustrating the surface physiography and tectonic structures of the African continent and adjoining oceans. The major volcanic edifices, large basins and plateaus are outlined and labelled in red. The major features of the East African rift system are indicated by the blue coloured dashed lines and labels. The associated volcanic peaks (Kenya and Kilimanjaro) are identified by red triangles. The green arrows indicated absolute plate velocities in a reference frame dominantly determined by Pacific hotspot tracks (Gripp and Gordon, 2002). The red arrows show absolute plate velocities in the Indo-Atlantic hotspot reference frame (Quéré et al., 2007).

asthenospheric flow and seismic anisotropy. An outstanding issue we consider is the relationship between flow patterns in the upper and lower mantle, and specifically on how the large-scale thermochemical upwelling 'domes' in the lower mantle (e.g. Davaille et al., 2005) evolve into more focussed, plume-like upwellings at shallower depths (e.g. Forte and Mitrovica, 2001). In this regard, we will elucidate the detailed connections between the predicted flow in the upper mantle and the surface distribution of late Cenozoic (and current) volcanism and surrounding basins.

2. Tomography based mantle flow model

We determine the convective flow field below the African plate using a Newtonian viscous flow model of the mantle (e.g. Richards and Hager, 1984) that incorporates internal buoyancy forces provided by joint seismic–geodynamic inversions for 3-D mantle structure. The flow predictions are based on a gravitationally consistent, compressible version of the governing fluid momentum equation in a spherical shell in which surface tectonic plates are coupled to the internal buoyancy-driven flow rather than being imposed *a-priori* (Forte and Peltier, 1991; Forte, 2007). These flow calculations require two fundamental inputs, namely the rheological structure of the mantle which we represent in terms of a depth-dependent effective viscosity and mantle density perturbations.

We employ mantle viscosity profiles inferred from joint inversions of global convection-related observables and glacial isostatic adjustment (GIA) data associated with the response of the Earth to melting of the Laurentian and Fennoscandian ice loads (Mitrovica and Forte, 2004). A significant characteristic of one such profile, model 'V1' (Fig. 2), is the relatively weak ($\sim 2\times10^{20}$ Pa s) viscosity in the asthenospheric mantle. Despite the nearly three order of magnitude increase in viscosity from the asthenosphere to the mid lower mantle, the average viscosity in the top ~1000 km of the mantle is close to 10^{21} Pa s, in accord with the Haskell constraint (Mitrovica, 1996).

The predicted mantle flow velocities, and the corresponding convection-related surface observables, are sensitive to the choice of mantle viscosity and we therefore consider a second GIA-convection-inferred viscosity profile, referred to as 'V2' (Fig. 2).The V2 viscosity profile yields similar fits to the GIA data as the V1 profile, though the low-viscosity notch at the base of the upper mantle is almost absent and it has a higher (by a factor of ~5) deep-mantle viscosity.

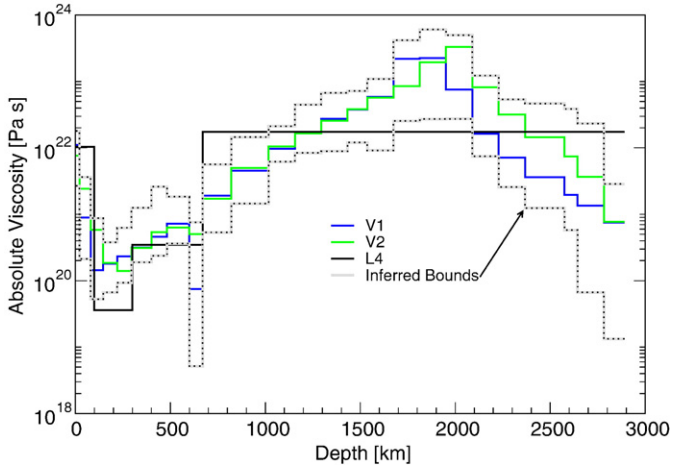

Fig. 2. Mantle viscosity structure employed in calculating mantle convective flow. The solid blue and green curves, labelled V1 and V2 respectively, are the depth-dependent effective viscosities derived in Occam-style inversions of combined glacial isostatic adjustment (GIA) and convection-related data sets (Mitrovica and Forte, 2004). The dashed grey lines illustrate the uncertainty in the viscosity inference determined by varying the smoothing weights in the Occam inversions. The solid black curve, labelled L4, is a four-layer model derived by Behn et al. (2004) from fitting mantle flow to seismically inferred anisotropy below the African plate.

We also consider a four-layer viscosity model, here referred to as 'L4' (Fig. 2), that was derived by Behn et al. (2004) on the basis of fitting tomography-based mantle flow predictions to inferences of seismic azimuthal anisotropy below the African plate. Although the value of lower mantle viscosity in L4 (17.5×10^{21} Pa s) is similar to the lower mantle–average value of V2 (19.4×10^{21} Pa s), it exceeds the joint GIA-convection-inferred viscosity bounds (grey curves, Fig. 2) at the top of the lower mantle. In the upper mantle, model L4 has a very low viscosity in the asthenosphere, 3.5×10^{19} Pa s, that also lies outside the inferred viscosity bounds. Additional analysis of these viscosity profiles is presented in the supplementary online materials.

The presence of lateral temperature variations associated with mantle convection will affect the microphysical mechanisms (e.g. diffusion) governing mantle creep rates (Poirier, 1985), thereby leading to large amplitude lateral viscosity variations (LVV) which will be superimposed on the effective radial variations we have inferred. A complex numerical treatment of buoyancy induced flow with 3-D viscosity variations (Forte et al., 1994; Moucha et al., 2007) has been carried out to evaluate the impact of global-scale LVV on predicted convection-related surface observables. Moucha et al. (2007) found that if the amplitude of the global-scale LVV is about 2 to 3 orders of magnitude, and comparable to that in the radial viscosity profile, the impact (measured in terms of variance reduction) on the predicted topography and geoid undulations is of the order of 25%. The impact of the LVV on mantle flow velocities will be stronger, mainly leading to a more sharply focussed pattern of upwellings and downwellings than is predicted with only radial viscosity variations and the mean amplitude of the horizontal components of flow can be changed by a factor of 2. Moucha et al. (2007) found that the impact of LVV on the predicted flow and surface observables is comparable to that arising from differences in the current seismic tomography models. These numerical simulations show that the locations and relative amplitudes of the vertical convective motions are essentially controlled by the distribution of mantle buoyancy and hence their geometry can be robustly mapped out with a simpler flow theory that assumes only a depth-dependent viscosity.

Density perturbations within the mantle were derived through a joint inversion of global seismic and geodynamic data sets in which mineral physical constraints on the thermal dependence of seismic wave velocities and density were explicitly incorporated (Simmons et al., 2007, 2009). These inversions are solved iteratively, with a starting model that assumes purely thermal anomalies. This constraint is then relaxed in subsequent iterations, when lateral variations in the density–velocity scaling are introduced, until an optimal reconciliation between the seismic and geodynamic constraints is obtained (for further details, see Simmons et al., 2009). The model is parameterised into spatial blocks defined by 22 layers extending from the core–mantle-boundary to the surface (with thicknesses ranging from 75 km to 150 km, except D" with 240 km thickness) and lateral dimension ~250 km.

The geodynamic data sets include global free-air gravity anomalies, crust-corrected inferences of dynamic surface topography, horizontal divergence of tectonic plate motions and the excess or dynamic ellipticity of the core–mantle boundary. Further details concerning these convection-related data sets may be found in Forte and Perry (2000) and Forte (2007). These geodynamic constraints are only sensitive to lateral variations in density relative to the mean (global horizontal average) radial variation of density in the mantle. Our flow calculations are formulated for a fully compressible mantle (Forte, 2007) and the mean density profile we employ is given by PREM (Dziewonski and Anderson, 1981).

The geodynamic data are jointly inverted with seismic data that include about 46,000 residual travel time measurements associated with seismic S, ScS, sS, sScS, SKS and SKKS phases as well as multi-

bounce surface multiples and shallow-turning triplicated phases (Grand, 2002; Simmons et al., 2007). These travel time data were obtained through synthetic waveform cross-correlations carried out for each individual measurement. The global seismic data in these new joint inversions include seismic phases measured in temporary seismic deployments in southern Africa (the Kaapvaal array), Tanzania and Ethiopia. The waves recorded by these African stations are important because they propagate through the South African superplume structure and thereby provide enhanced constraints on this significant lower mantle feature which is known to possess extreme lateral velocity gradients and other complexities (Ritsema et al., 1999; Ni et al., 2002; Ni et al., 2005).

In this study we focus on two tomography models derived from the joint seismic–geodynamic inversions: TX2007 (Simmons et al., 2007) and TX2008 (Simmons et al., 2009), in which the latter employs stronger smoothing constraints in the inversions relative to the 2007 model. Both models TX2007 and TX2008 fit the global seismic shear wave travel time constraints to within 96% and 93%, respectively, similar to that obtained with previous purely travel time derived models such as TX2002 (Grand, 2002). However, as discussed below, the fits to the convection-related data over Africa (and globally) yielded by these new 3-D mantle models are substantially improved relative to those previously obtained with tomography models obtained by inverting seismic data alone (e.g. TX2002).

The joint seismic–geodynamic inversions are formulated such that the scaling coefficient between perturbations of density and seismic shear wave velocity varies both radially and laterally thereby allowing an explicit mapping of the 3-D contributions to mantle density anomalies that have both thermal and chemical origins (Simmons et al., 2007, 2009). The globally averaged rms amplitudes of the compositional and thermal contributions to density anomalies show that the latter dominate throughout the mantle (see Supplementary Fig. S2). The thermal contributions follow mineral physical constraints on the relationship between density and seismic shear velocity anomalies (Fig. S2). The compositional (non-thermal) anomalies are derived by subtracting the thermally controlled density anomalies from the total 3-D density anomalies inferred by the joint seismic–geodynamic inversions (Simmons et al., 2007, 2009). The core of the South African superplume structure is characterised by a positive chemical density anomaly that opposes the thermally-induced density perturbations (e.g. Simmons et al., 2007). As we show below, this compositional anomaly strongly reduces the total integrated buoyancy of the South African superplume.

3. African mantle dynamics and surface geodynamic observables

The degree to which we can be confident of the mantle flow predictions obtained from the tomography-based convection models depends on the extent to which these models can satisfactorily fit the main convection-related surface data sets. These data sets include the global surface gravity anomalies, tectonic plate motions, crust-corrected inferences of dynamic topography, and excess (non-hydrostatic) ellipticity of the core–mantle boundary. A detailed review of these data sets and their use in constrainingtomography-based calculations of mantle dynamics may be found in Forte (2007). These surface geodynamic data provide fundamental constraints on density anomalies throughout the mantle and hence on the buoyancy forces that drive the convective flow.

We consider here the geodynamic fits provided by a number of tomography-based convection calculations that also include a previous global shear wave tomography model, S20RTS, derived by Ritsema et al. (1999), in addition to the joint seismic–geodynamic tomography models TX2007 and TX2008 discussed above. The S20RTS model has been widely used in past studies of African mantle dynamics (e.g. King and Ritsema 2000; Gurnis et al., 2000; Daradich et al., 2003; Conrad and Gurnis 2003; Behn et al., 2004). The geodynamic calculations presented here will explore the variability in the predicted convection-related observables arising from different inferences of the 3-D density and radial viscosity structures in the mantle.

We first review the global data fits (Table 1) because the tomography-based convection models are fully global in extent. The fits in the geographic region occupied by the African plate (Fig. 1) will be discussed below. The previous tomography-based investigation of mantle dynamics below the African plate, by Behn et al. (2004), incorporated the L4 viscosity model (Fig. 2) and density anomalies derived from the S20RTS tomography model (Ritsema et al., 1999). The fits to the geodynamic observables provided by this flow model and an earlier tomography-based flow model by Forte and Mitrovica (2001) are reviewed in the Supplementary materials. We have attempted to maximise the fits provided by the S20RTS tomography model, in a plate-coupled flow calculation, by carrying out Occam-style inversions for optimal density–velocity conversion profiles (see Supplementary Fig. S2). A discussion of this Occam inversion procedure may be found in Forte (2007). With these inverted conversion profiles, the S20RTS model yields fits to the global free-air gravity anomalies and dynamic surface topography (rows 1 and 2, Table 1) that are comparable to those obtained with other purely seismic tomography models (Forte, 2007).

The global data fits provided by TX2007 and TX2008 are excellent (last 2 rows in Table 1), yielding almost complete matches to the global geoid and plate motion data, and greatly improved fits to the global gravity and topography constraints. A detailed review of global geodynamic fits provided by a suite of previously published tomography models is presented in Forte (2007). In the context of these earlier results, we note that the new tomography models (TX2007/2008) provide greatly improved fits to the convection-related data sets while achieving a successful reconciliation between the independent seismic and geodynamic constraints on 3-D mantle structure.

The fits provided by the tomography-based convection models to the geodynamic data in the region of the African plate (Fig. 1) are summarised in Table 1. Figs. 3 and 4 show the African gravity and dynamic topography fields predicted on the basis of the optimised treatment of density conversion in model S20RTS and the joint

Table 1
Fits[a] between predicted and observed[b] convection-related data.

Mantle Convection Model	Global Geoid / Gravity[c]	Global Dynamic Topography	Global Plate Velocities	African Geoid / Gravity[c]	African Dynamic Topography	African Plate Velocity
S20RTS + L4INV[d]	5%/19%	18%	50%	21%/13%	47%	53%
S20RTS + V2INV[e]	54%/24%	34%	53%	32%/14%	43%	46%
TX2007 + V1[f]	91%/69%	59%	92%	84%/57%	53%	86%
TX2008 + V2[g]	90%/65%	64%	95%	89%/59%	62%	93%

[a] All fits are quantified in terms of percent variance reduction. Unless stated otherwise, all predictions and data are represented by a sum of spherical harmonics to maximum degree and order 32. The 'African' fits refer to the geographic region in Fig. 1.
[b] All data sets are described in Forte (2007).
[c] The first value is the variance reduction to the non-hydrostatic geoid and the second is for the corresponding free-air gravity anomalies.
[d] Mantle density is derived from the S20RTS tomography model and 'L4 INV' density–velocity conversion (dashed blue curve, Supplementary Fig. S2a). Mantle flow is calculated using the 'L4' viscosity profile (black curve, Fig. 2).
[e] Mantle density is derived from the S20RTS tomography model and 'V2 INV' density–velocity conversion (dash–dotted blue curve, Supplementary Fig. S2a). Mantle flow is calculated using the 'V2' viscosity profile (green curve, Fig. 2).
[f] Mantle density is derived from the TX2007 tomography model, including both thermal and compositional contributions (solid red and green curves, Supplementary Fig. S2b). Mantle flow is calculated using the 'V1' viscosity profile (blue curve, Fig. 2).
[g] Mantle density is derived from the TX2008 tomography model, including both thermal and compositional contributions (dashed red and green curves, Supplementary Fig. S2b). Mantle flow is calculated using the 'V2' viscosity profile (green curve, Fig. 2).

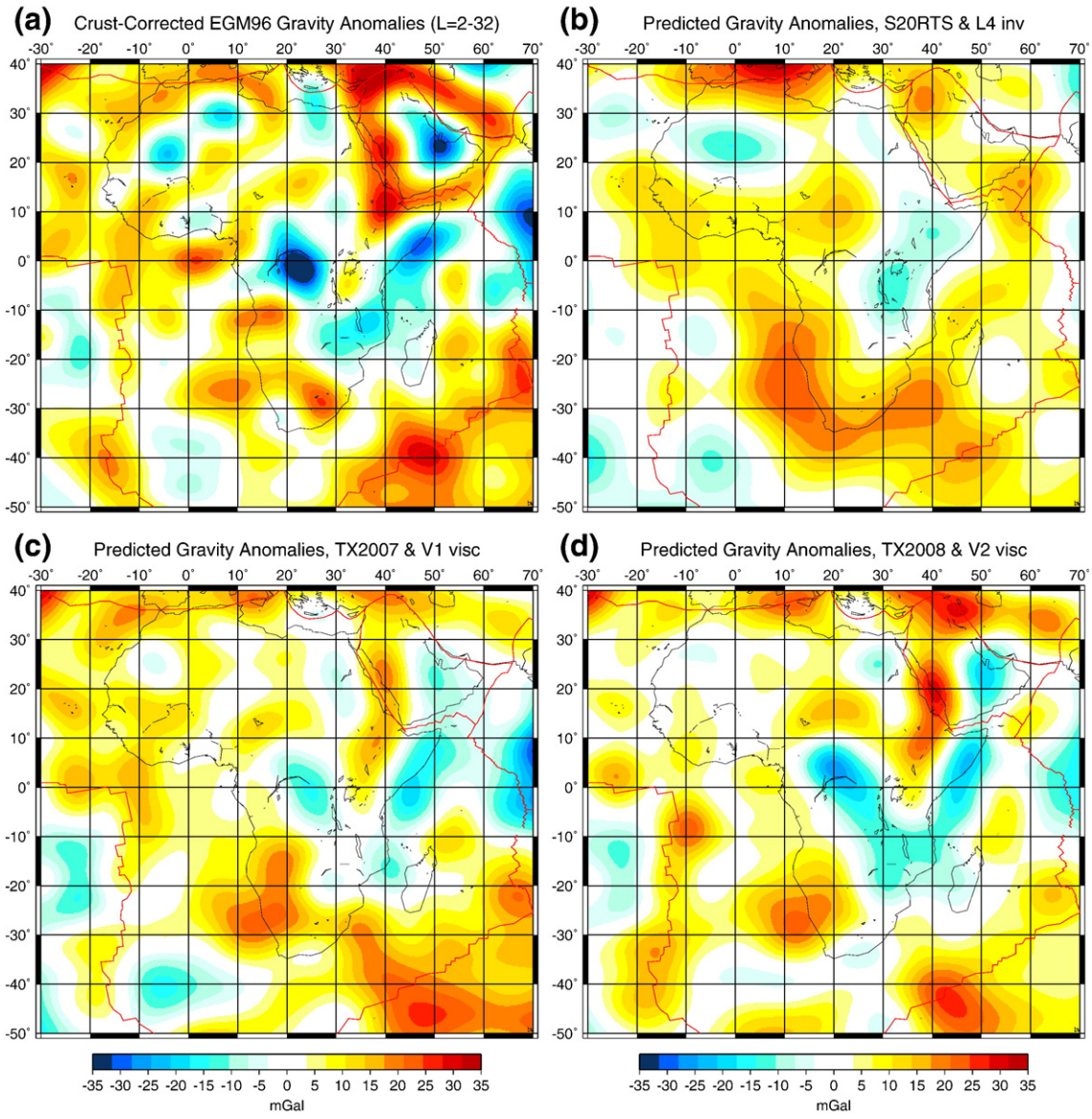

Fig. 3. African free-air gravity anomalies. (a) Free-air gravity anomalies derived from the EGM96 geopotential model (Lemoine et al., 1998) and corrected by removing the gravitational signal of isostatically compensated crust (see Suppl. Fig. S3f). (b) Gravity anomalies predicted with the S20RTS tomography model, 4-layer viscosity model (black curve, Fig. 2) and corresponding inverted density-velocity conversion (dashed blue curve, suppl. Fig. S2a). (c) Gravity anomalies predicted with the density anomalies in the TX2007 tomography model (solid red and green curves, suppl. Fig. S2b) and the V1 viscosity profile (blue curve, Fig. 2). (d) Gravity anomalies predicted with the density anomalies in the TX2008 tomography model (dashed red and green curves, suppl. Fig. S2b) and the V2 viscosity profile (green curve, Fig. 2). All flow calculations have coupled, convection-driven surface plate motions and the gravity fields are mapped up to spherical harmonic degree and order 32.

seismic–geodynamic tomography models TX2007 and TX2008. In this case all observables and predictions are presented up to harmonic degree 32. A quantitative summary of the fits to the African geodynamic data is provided in Table **1** (rows 1 and 3–4). Although the fit to the dynamic topography constraints provided by model S20RTS is significantly improved (compare Fig. 4a,b), there remains a significant misfit between predicted and observed gravity anomalies (compare Fig. 3a,b) over eastern Africa and the adjoining portion of the Indian Ocean that includes the Somali Basin (Fig. 1). Models TX2007 and TX2008 provide equally good fits to both the free-air gravity (compare Fig. 3a,c,d) and dynamic topography (compare Fig. 4a,c,d) data sets.

As emphasised at the beginning of this section, the differences in mantle density structure revealed by the differing degrees of fit to the surface geodynamic constraints can have significant consequences for the buoyancy-driven mantle flow. A further exploration of this issue is presented in the Supplementary online materials, Fig. S4 where we show the sensitivity of the vertical and especially the horizontal flow to the choice of tomography-based density structure in the mantle.

4. Superplume-driven mantle flow below the African plate

We now consider the detailed characteristics of the mantle flow under the African plate predicted on the basis of the density anomalies in model TX2007 and using the V1 viscosity inference (Fig. 2, blue curve). For the purpose of the mantle flow calculations, the total (thermal plus chemical) density anomalies (see Fig. S2b) and the corresponding buoyancy-driven flow are represented, at all depths, in terms of a spherical harmonic expansion up to degree and order 128. The minimum horizontal scale resolved by this harmonic expansion is ~160 km at the surface, thereby allowing a full representation of the short-wavelength structural variations in TX2007. The radial variation

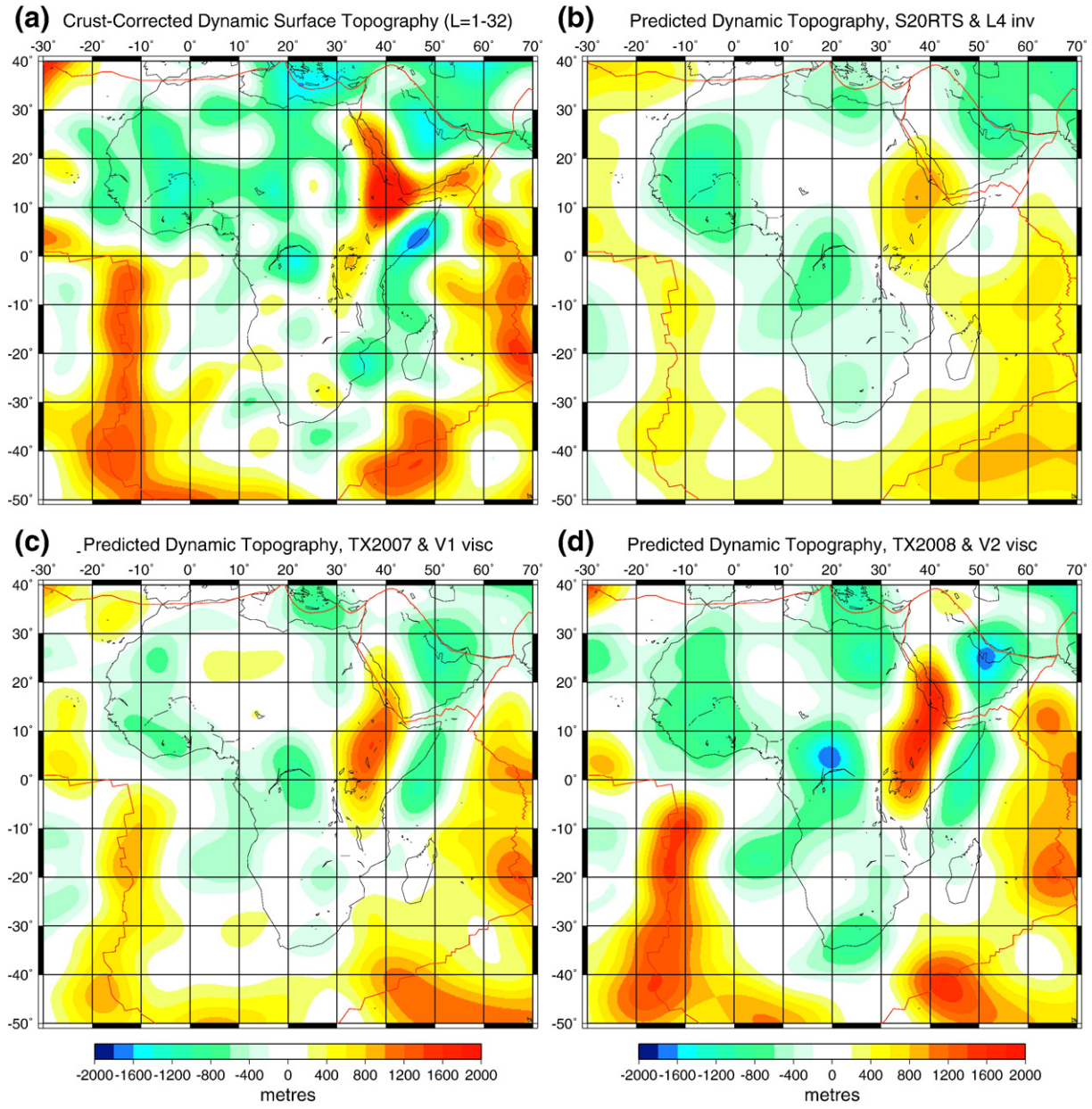

Fig. 4. African dynamic topography. (a) Dynamic (non-isostatic) topography inferred by removing isostatically compensated crustal topography from the observed topography (see Supplementary Fig. S3j). (b) Dynamic topography predicted with the S20RTS tomography model, 4-layer viscosity model (black curve, Fig. 2) and corresponding inverted density–velocity conversion (dashed blue curve, Supplementary Fig. S2a). (c) Dynamic topography predicted with the density anomalies in the TX2007 tomography model (solid red and green curves, Supplementary Fig. S2b) and the V1 viscosity profile (blue curve, Fig. 2). (d) Dynamic topography predicted with the density anomalies in the TX2008 tomography model (dashed red and green curves, Supplementary Fig. S2b) and the V2 viscosity profile (green curve, Fig. 2). All flow calculations have coupled, convection-driven surface plate motions and the topography fields are mapped up to spherical harmonic degree and order 32.

in the mantle flow field is parameterised in terms of Chebyshev polynomials up to order 65, yielding a maximum radial resolution of ~70 km at mid-mantle depth.

A fluid-mechanical interpretation of the 3-D seismic structure under the African plate (Davaille et al., 2005), based on comparisons of the morphology of this structure with that found in thermochemical convection experiments in the laboratory, has suggested three large-scale upwelling 'domes' in the lower mantle located below: (i) southern Africa, below the surface location of the corresponding 'superswell' (Nyblade and Robinson, 1994); (ii) western equatorial Africa, below the surface locations of the CapeVerde and Canary Islands; and (iii) southwest Indian Ocean under Crozet, Marion and Kerguelen Islands. Tomography-based mantle flow modelling has previously yielded maps of very broad-scale lower mantle upwellings under these three regions (e.g. Forte, 2000, Forte and Mitrovica, 2001; Behn et al., 2004), but the resolution of the previous tomography models did not provide a sufficiently clear delineation of the individual upwellings postulated by Davaille et al. (2005). With the new higher resolution inferences of thermochemical heterogeneity in the tomography models TX2007 and TX2008, we can now carry out flow calculations that directly incorporate the short-wavelength structure in these models thereby allowing a detailed mapping of mantle flow at all depths.

We first consider the mantle flow predicted under the South African 'superswell'. The large-scale and intensity of the mantle upwelling we predict under this region motivate us to employ the appellation 'South African Superplume' (henceforth 'SASP'). The flow patterns associated with the SASP are plotted on two orthogonal cross-

sections: one following the SW–NE axis of the African Rift system (Fig. 5a) and the other following a W–E traverse of the Kalahari craton (Fig. 5b). The central axis of the large-scale upwelling originating deep in the lower mantle appears to lie directly below the Kalahari craton and this flow then diverges laterally around the cratonic root as it enters the upper mantle (Fig. 5b). We note that it is the combination of the northeasterly tilt of the SASP and its compositional buoyancy at mid-mantle depths (Fig. 5a) that results in the most active centre of vertical mid-mantle flow below South Africa rather than under the East African Plateau, as in the flow calculated with S20RTS (Behn et al., 2004). The geometry of the flow field driven by the SASP is essentially sub-horizontal throughout most of the upper mantle below the African Rift system (Fig. 5a) and it is characterised by flow rates that are much greater than those of the overlying African plate motion. This marked contrast between the observed surface tectonic plate movement and the sublithospheric flow field is controlled by the substantial reduction of viscosity in the asthenospheric mantle (Fig. 2).

The character of the flow field changes substantially in the W–E equatorial section passing through the East African Plateau (Fig. 5c). Here we note that deep-seated thermal buoyancy in the mid-mantle is again offset by compositional buoyancy and, as a result, the most significant vertical flow rates are confined to the upper mantle, above ~400 km depth. A small-scale, edge-driven style of convection (King and Ritsema 2000) in the shallow mantle, west of the African cratonic lithosphere, is evident in the predicted flow field (Fig. 5b,c). This near-surface flow field constitutes a second scale of convection that is superimposed on the dominant large-scale flow driven by the deep-mantle superplume. The most significant activity (Fig. 5c) is focussed below the eastern flank of the East African Plateau, under the Eastern Rift, where the local vertical flow is strongest. As discussed further below, this focussed shallow upwelling could be a candidate source region for the Kenya volcanic domes.

A particularly noteworthy aspect of the flow field is the strong, eastward dipping mantle downwelling that extends deep under the Somali basin in the Indian Ocean (Fig. 5c). This quasi-linear downwelling, characterised by a near-surface flow trajectory that resembles that of a shallow-dipping subduction zone, appears to be a mechanism for accommodating the opening of the East African Rift.

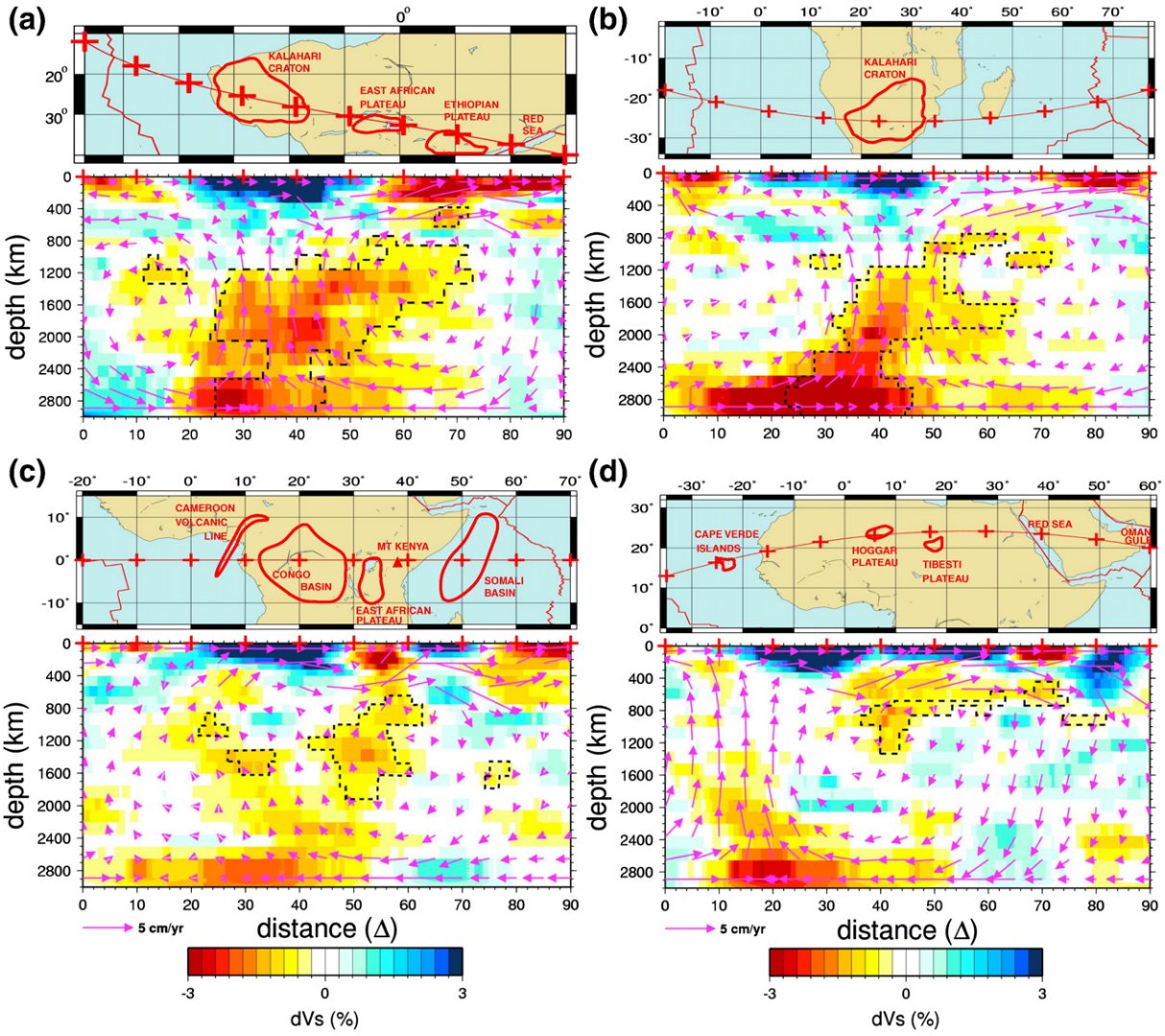

Fig. 5. Mantle convective flow below the African plate. Each frame (a–d) contains a vertical mantle cross-section passing through the African continent. The geographic location of each cross section is shown by the red curve in the superimposed map frames and the red crosses spaced at 10° intervals mark the surface locations shown in the underlying cross-section frames. The coloured blocks in the cross-sections (colour scale at bottom) show the seismic shear velocity anomalies from theTX2007 tomography model. The dashed black lines enclose mantle regions in which the chemical density anomaly exceed +0.1%. The magenta arrows superimposed on the seismic velocity anomalies show the mantle flow velocities (arrow scale at bottom left)predicted on the basis of the total (thermal + chemical) buoyancy (Supplementary Fig. S2b, solid red and green curves) and V1 viscosity (Fig. 2). Note: the vertical depth scale is exaggerated (×13) relative to the horizontal scale.

This 'rift-accommodating' Somali downwelling is analogous to the downwelling predicted under the eastern margin of the Arabian plate that contributes to the opening of the Red Sea (Fig. 5d).

A second major mantle upwelling, with a scale and intensity rivalling that of the SASP, is localised below West Africa (Fig. 5d). In the tomography-driven flow the central axis of this West African superplume (henceforth 'WASP') lies below the Cape Verde Islands. The upwelling driven by the WASP diverges laterally upon reaching the base of the West African cratonic root, driving a strong sub-horizontal flow eastward. A remarkable aspect of the convective flow below northern Africa is the large plume-like structure that appears to lie below the Hoggar massif that possibly extends to the Tibesti dome (see also Supplementary Fig. S8). This 'Hoggar plume' lies below a region of significant thinning of the continental lithosphere (Fig. 5d) and it has been previously suggested that this is analogous to the thermal structure of mid-oceanic (e.g. Bermuda) swells (Crough 1981). The eastward moving Hoggar plume head appears to be detached from a source region in the lower mantle which may have been the same as that currently feeding the WASP. A possible connection between the source region of the North African volcanic domes and the source of volcanic activity on the Cape Verde and perhaps Canary Islands has been inferred previously on the basis of geochemical analyses of basalts extracted from these localities (Allegre et al., 1981).

The third postulated lower mantle upwelling dome (Davaille et al., 2005), under the southwest Indian Ocean portion of the Antarctic plate, is not shown in the cross-sections in Fig. 5, however it is somewhat evident (in map view) in Fig. 6c and its near-surface expression is also discernable (albeit with a lateral displacement) in

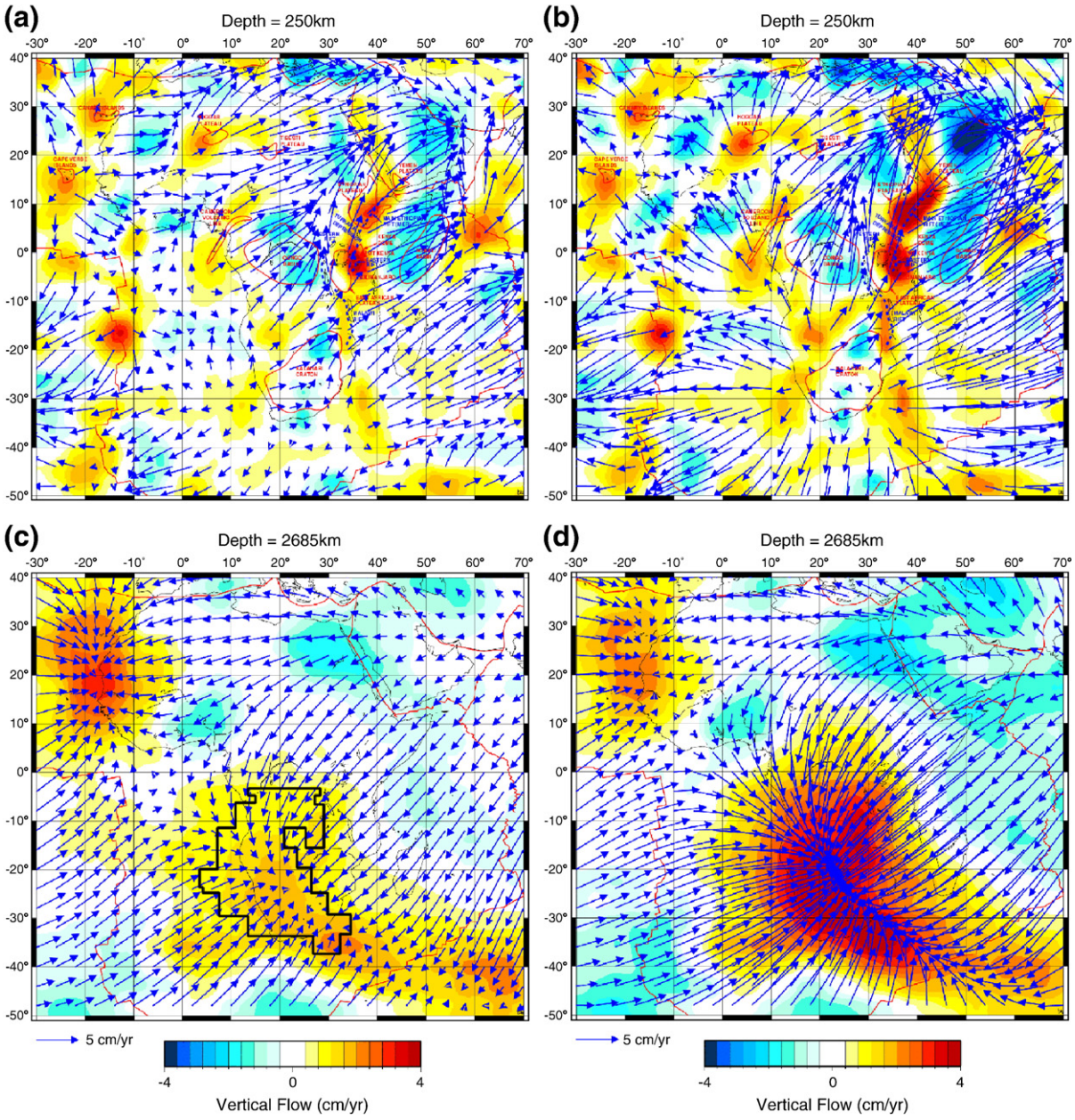

Fig. 6. Predicted mantle convective flow below the African plate. (a) The predicted rates of horizontal (arrows) and vertical (contours) flow at a depth of 250 km are obtained from the same viscous flow calculation shown in Fig. 5.The major surface physiographic features (volcanic plateaus, and basins) identified in Fig. 1 are outlined in magenta. (b) Flow predicted at 250 km depth when all chemical buoyancy in the SASP (Figs. 5a,b) is set to zero. (c) As in (a), except the flow is shown at a depth 2685 km (a couple of hundred kilometres above the CMB). The dark black polygon encloses those portions of the mantle in which the chemical density anomaly (Fig. 5a,b) exceeds +0.1%. (d) Flow predicted at2685 km depth when all chemical buoyancy in the SASP is set to zero.

Fig. 6a. The strength of the predicted upwelling is relatively muted in comparison to that of the SASP and WASP. Some caution is required in interpreting the predicted lower mantle flow in this region, because standard seismic ('checkerboard') resolution tests (Simmons, 2007) show that seismic ray coverage of the lowermost mantle under the southwest Indian Ocean is weak.

To understand the origin and evolution of the large-scale anomalies in the lower mantle that have been resolved by seismic tomography, a number of purely numerical thermal convection simulations have been performed, incorporating the estimated 120 million year history of tectonic plate motions as a surface boundary condition (e.g. Bunge et al., 2002; McNamara and Zhong, 2005; Quéré and Forte, 2006). These simulations reveal that the rather stable 'horse-shoe' pattern of descending cold material under the circum-Pacific system of subduction zones over the past 120 Ma, has organised the hot upwelling thermal anomalies at the base of the mantle into nearly stationary 'hotlines': one under the central Pacific and the other under Africa. The detailed evolution of these hotlines is sensitive to unknown initial conditions (at 120 Ma) and uncertainties in: the history of Mesozoic and Cenozoic plate motions, mantle viscosity, internal heating rates, and the amplitude of stabilising chemical heterogeneity at the base of the mantle (e.g. Bunge et al., 2002; McNamara and Zhong, 2005; Quéré and Forte, 2006).

Despite these complexities, it is nonetheless possible to obtain an initial understanding of the origin of the deep-mantle thermal anomalies under the African plate. In Supplementary Fig. S5 we compare temperature anomalies at 2800 km depth derived from the thermal component of model TX2007 with the corresponding anomalies predicted by the purely numerical convection model of Quéré and Forte (2006). We note (Supplementary Fig. S5b) that the convection model predicts a strongly developed linear thermal structure connecting a focussed anomaly under the Cape Verde Islands (the base of the WASP) to a similarly focussed anomaly under the southwest Indian Ocean, passing through the base of the SASP. The overall amplitude of the temperature anomalies predicted by the convection model is in accord with that derived from the thermal component of model TX2007 (in Supplementary Fig. S5a). We note that the spatial extent of the thermal anomaly at the base of the SASP predicted by the thermal-convection model is time-dependent and hence sensitive to the particular instant chosen in the simulation (see Supplementary Fig. S5c). The convection simulations of McNamara and Zhong (2005) also point to the possible role of chemical piles at the CMB in controlling the horizontal extent of the SASP. In contrast to the robustness of the lower mantle hotline below the western margin of the African continent, the second hot line passing under the northern and eastern margin of the African plate is a transient (i.e. non-steady state) feature (compare Figs. S5b,c) whose presence is also quite sensitive to assumptions about internal heating and mantle viscosity (Quéré and Forte, 2006).

5. Impact of deep buoyancy on African plate motion and asthenospheric flow

It thus appears that mantle flow dynamics below the African plate are dominated not by a single superplume, the SASP, as is generally assumed, but the combined contributions from the SASP and WASP. To further investigate the dynamical importance of these two superplumes we consider their contributions to the driving forces responsible for African tectonic plate motion. The plate motions resulting from the mantle flow generated by all buoyancy sources in the mantle are shown in the supplementary online materials (Supplementary Fig. S6). The mantle flow contributions to African plate motion resulting from the SASP may be tested by removing all buoyancy in this superplume, in a region extending vertically from the core–mantle boundary (CMB) to the lithosphere and extending horizontally from the southern tip of Africa to the Red Sea (i.e. the red-yellow coloured region in Fig. 5a). The consequences for African plate motion are shown in Supplementary Fig. S6 (blue arrows) and the corresponding perturbation in the rotation rate vector of the African plate is 35%. We note that the motion of the Arabian plate is strongly impacted by the removal of the SASP buoyancy. If we instead remove all buoyancy in the WASP (red-yellow coloured region in Fig. 5d below the Cape Verde Islands that extends down to the CMB) the impact on the surface plate motion is shown in Supplementary Fig. S6 (red arrows) where the change in the African plate rotation vector is 31%. The dynamical impact of WASP and SASP buoyancy on African surface plate motion are comparable and this underlines the importance of the WASP on African mantle dynamics.

The dynamic importance of the WASP (Fig. 5d) is dependent on its strong thermal buoyancy, in contrast to the SASP which is modulated by opposing chemical buoyancy (Fig. 5a and b). To quantify the strong stabilising control of the chemical component of SASP buoyancy on mantle flow below Africa, we have carried out a convection simulation in which all density perturbations in the SASP due to chemical heterogeneity (green curve in Supplementary Fig. S2b) are set to zero. As expected, the impact on deep-mantle flow dynamics is strong (compare Fig. 6c,d), to the extent that the lower mantle upwelling due to the SASP is strongly amplified and dominates the WASP in the absence of chemical buoyancy. The dynamical control of deep-mantle chemical buoyancy also extends to the asthenosphere (Fig. 6a,b), with the strongest impact evident on the horizontal pattern of asthenospheric flow under most of Africa. In the absence of opposing chemical buoyancy, the asthenospheric flow radiates outward in all directions from a region in the shallow mantle under the Kalahari craton that lies above the central portion of the SASP (Fig. 6b).

The predicted convective flow in the asthenosphere (Fig. 6a) shows detailed correlations with all major centres of late Cenozoic volcanic activity on the African continent (Thorpe and Smith, 1974; Burke, 1996). The origin of these shorter wavelength aspects of sublithospheric flow is due to two factors: the low asthenospheric viscosity inferred from the joint convection and GIA data (Fig. 2) and the resolution of short wavelength upper-mantle structure below Africa in model TX2007. The strongest centres of vertical upwelling below the African Rift Valley system lie directly below Ethiopia and the Kenya Dome, east of the Tanzania Plateau. These two upwellings are separated by a gap that appears to lie under the Turkana depression (Fig. 1). The significance ofthis gap is unclear since model TX2007 incorporates data collected from portable seismic arrays in Tanzania, Kenya and Ethiopia, but no stations were deployed in the Turkana region. The shallow upwelling centres beneath the East African Rift system (EARS) are part of a much larger scale pattern of flow that is driven by the SASP (Fig. 5a).

The predicted asthenospheric upwelling under the Main Ethiopian Rift (MER) is interesting in the light of the most recent high-resolution regional tomography by Bastow et al. (2008). This regional P- and S-wave imaging study under the MER found that the lowest seismic velocities in the asthenosphere are centred not beneath Afar, but rather at about 9° N, 39° E. This location coincides with the maximum vertical flow rate we predict at 250 km in the same region (Fig. 6a). Our (global) mantle flowpredictions thus yield detailed flow patterns that accord with local imaging of seismic anomalies under the Ethiopian Rift system. This agreement supports the hypothesis (Bastow et al., 2008) that the negative velocity anomalies under Ethiopia are the result of decompression melting due to buoyancy-driven vertical flow in the asthenosphere.

It is noteworthy that the amplitude of the asthenospheric upwelling below the EARS is comparable to that below the mid-Atlantic ridge and that it can be clearly delineated southward until it intersects the location of the Africa–Antarctica plate boundary. Well defined upwelling centres are also evident (Fig. 6a) under the Hoggar and Tibesti massifs in North Africa, the Cape Verde and Canary Islands, the Cameroon volcanic line, and a region extending from southern Angola to northern Namibia.

The pattern of asthenospheric flow reveals that the shallow mantle under the Congo Basin is almost entirely surrounded by mantle upwellings. This quasi-circular pattern of upwelling flow drives a well defined sublithospheric downwelling below the Congo Basin. The predicted downwelling under the Congo is, in effect, 'accommodating' (as required by simple mass conservation) the buoyant mantle upwellings that surround this region, similarly to the accommodation described above under the Somali basin (Fig. 5c) and also under the Gulf of Oman (Fig. 5d). This downwelling flow and the associated surface dynamic stresses should provide strong control on the evolution and depth of this sedimentary basin, in accord with previous geodynamic hypotheses (Sahagian 1993; Hartley and Allen 1994).

6. Implications for asthenospheric deformation and seismic anisotropy

Studies of mantle seismic anisotropy under the African continent and surrounding oceans provide important constraints on mantle flow patterns and regional variations in tectonic setting (Vinnik et al., 1995; Silver, 1996; Barruol and Ben Ismail, 2001). The geodynamic significance of these anisotropy constraints has motivated previous tomography-based convection simulations of the flow-induced deformation of the shallow mantle under the African and adjacent plates (Behn et al., 2004). The two principal seismic techniques employed to map African anisotropy are shear wave splitting analyses (Vinnik et al., 1995; Barruol and Ben Ismail 2001; Silver et al., 2001; Walker et al., 2004; Gashawbeza et al., 2004; Kendall et al., 2005; Hammond et al., 2005; Hansen et al., 2006) and azimuthal anisotropy inferred from surface waves (Hadiouche et al., 1989; Sebai et al., 2006) that, respectively, provide detailed local-scale and longer wavelength inferences of flow-induced orientation of mantle fabric.

We therefore explore the implications of our tomography-based convection model by considering the relationship between seismic inferences of anisotropy beneath the African plate and our predicted mantle flow patterns. This investigation requires that we employ suitable approximations for the lattice-preferred orientation (LPO) of mantle minerals in terms of appropriate representations of the flow-induced deformation field in the mantle. We consider here two simplified proxies for seismic anisotropy in the mantle, namely the mantle flow vector or, alternatively, the principal axis of the strain-rate tensor corresponding to the direction of greatest stretching or extension (Gaboret et al., 2003). This maximum strain-rate axis has been used to obtain a first-order estimate of preferred orientation under the Pacific plate (Gaboret et al., 2003) and under the oceanic portions of the African plate (Behn et al., 2004). It is important to briefly consider whether there is a sufficient basis for the use of either of these two proxies.

The existence of a direct correlation between mantle flow directions and seismic anisotropy due to lattice preferred orientation (LPO) of olivine grains in the upper mantle has long been assumed since the connection was first proposed by Hess (1964). The underlying mineral physical and fluid-mechanical conditions that justify the assumption of a simple connection between flow direction and anisotropy have not been clearly established. The complexity of this connection has been underscored by a number of theoretical (e.g. McKenzie, 1979; Ribe, 1992; Kaminski and Ribe, 2002) and experimental (e.g. Zhang and Karato 1995) studies that have related seismic anisotropy to the state of finite strain (and the history of deformation) of the mineral grains in the convecting mantle. These studies suggest that an interpretation of LPO and seismic anisotropy in terms of the principal axes of the finite-strain tensor is more relevant than a characterisation in terms of mantle flow directions.

Kaminski and Ribe (2002) have analysed the circumstances under which the mantle flow directions and maximum strain-rate axes may be related to the LPO of olivine and hence to seismic anisotropy. For simple plane strain deformations, they find that the fast a-axes of a deforming olivine aggregate will rotate towards the orientation of the infinite strain axis and that for *simple* shear this will also be aligned with the flow direction (and the a-axes will be rotated by 45° relative to the axis of maximum strain rate). In contrast, for *pure* shear the infinite strain axis and hence the LPO will evolve to an orientation that is co-linear with the maximum strain-rate axis.

For more general, non-uniform 3-D flow patterns, Kaminski and Ribe (2002) considered the necessary conditions for the alignment of LPO with the flow direction and they derived a local dimensionless 'grain orientation lag' parameter, Π, that can be used to quantify the degree to which this alignment obtains. They find that when Π is sufficiently small (typically less than 0.1) the LPO rotates toward the flow direction. If $\Pi > 0.5$, as in the vicinity of mantle upwellings (e.g. ridges or plumes), then there is no simple relationship between local flow and the orientation of the fast a-axis of olivine. This complexity should be kept in mind when considering the flow-anisotropy correlations we present below.

Previous inferences of deformation under southern Africa from seismic shear wave splitting have been interpreted in terms of present-day mantle flow (Vinnik et al., 1995) or in terms of preserved structures in the cratonic lithosphere (Silver et al., 2001).To test these interpretations we explore the plausibility of relating present-day mantle deformation in the African asthenosphere to seismic anisotropy inferred from SKS splitting analyses. As a working hypothesis, we shall assume that the predicted mantle flow at 250 km depth is sufficiently deep to avoid the complexity associated with potential rheological channelling of the flow under the continental lithosphere proposed by Ebinger and Sleep (1998).

The predicted pattern of athenospheric flow and maximum horizontal stretching in Fig. 7 show complex regional changes across the African plate. We begin by comparing these flow predictions to the azimuthal anisotropy inferred across the African plate by Barruol and Ben Ismail (2001) on the basis of splitting analyses of teleseismic shear waves. A summary of the angular relationship between the SKS splitting axes (magenta lines, Fig. 7) and the horizontal components of mantle flow (blue vectors, Fig. 7) are presented in a histogram in Supplementary Fig. S7a. A histogram summarising the relationship between anisotropy and the horizontal stretching rates (green lines, Fig. 7) is presented in Supplementary Fig. S7b. These histograms show well defined peaks for angular deviations less than 20°, but also 'tails' extending to greater angular misfits. These tails can be indicative of complexity in mantle deformation that invalidate a simple connection between LPO and the proxy flow indicators we employ, as discussed in Kaminski and Ribe (2002). They may also indicate the possible presence of 'frozen' anisotropy in the lithosphere that is not simply related to present-day flow in the asthenosphere. Additional complicating factors may be the presence of hydrated minerals and the generation of partial melts in zones of strong asthenospheric upwelling, as discussed in Karato et al. (2008).

The possible correlation between the SKS splitting magnitudes and mantle deformation rates is explored in terms of linear regression fits that are summarised in Supplementary Fig. S7c. The residuals relative to these hypothetical linear fits (open squares, Supplementary Fig. S7c) are of the order of 0.5 s and, as discussed above, they may reflect complications from a number of causes, including fossil anisotropy in the crust and lithosphere, shape-preferred orientation, partial melting, and strong lateral viscosity variations. The importance of these possible mechanisms will clearly vary depending on the tectonic context (e.g. cratonic versus current active rifting sites). On the whole, these analyses suggest an important, if not dominant, contribution to SKS splitting from present-day flow-induced deformation in the African asthenosphere.

We next consider the local, regional-scale relationship between the predicted flow and deformation and seismic anisotropy in each of the four regions identified on the map in Fig. 7. Region (I) involves a detailed comparison with the splitting analyses of Walker et al. (2004)

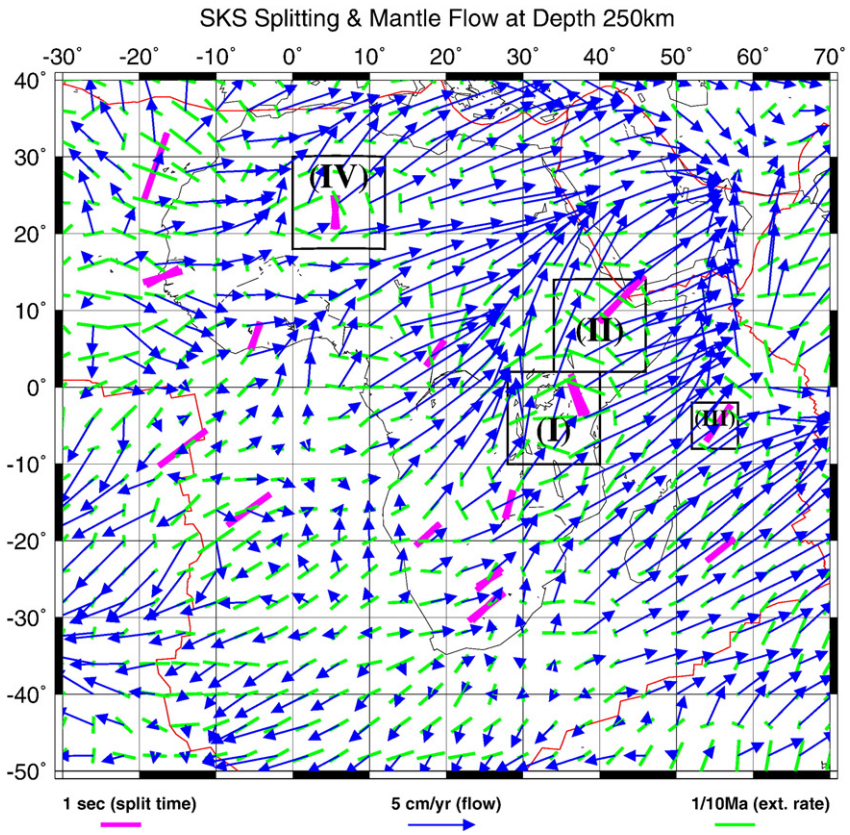

Fig. 7. Convection-induced deformation in the African asthenosphere. The magenta lines represent inferences of seismic anisotropy (scale bar at bottom of figure) determined by SKS splitting analysis carried out by Barruol and Ben Ismail (2001).The green lines (scale at bottom of figure) represent predictions of the horizontal component of maximum stretching (corresponding to the largest eigen value of the strain-rate tensor) at 250 km depth. The blue arrows represent the horizontal component of mantle flow predicted at 250 km depth. These predictions of sublithospheric flow and deformation are obtained from the same flow calculation employed in Fig. 5. The black boxes labelled '(I)' to '(IV)' identify regions where a detailed comparison betweenflow and seismic anisotropy is carried out in the supplementary online materials (see Supplementary Fig. S8).

in East Africa and is shown in Fig. S8 of the Supplementary online materials. In Region (II) (see Supplementary Fig. S8), we compare the predicted flow and deformation under the Ethiopian Rift with the splitting analyses of Gashawbeza et al. (2004). A flow comparison with the splitting measurements in the Seychelles obtained by Hammond et al. (2005), in Region (III), is interesting (see Supplementary Fig. S8) because this region is located above a local upwelling (akin to a diffuse 'corner flow') generated on top of the cold ('slab'-like) Somali downwelling as shown in Fig. 5c. Finally, in Region (IV) we have a close-up view of the predicted flow regime associated with the focussed upwelling under the Hoggar Plateau (Supplementary Fig. S8). In each of these regions we explore the possible impact of strong local reductions in asthenospheric viscosity (due to the temperature dependence of mantle viscosity) by also presenting mantle flow predictions obtained with the L4 viscosity profile (black curve in Fig. 2).

The deformation field under the EARS as shown in Fig. 7 (see also Regions (I) and (II) in Fig. S8) is characterised by a local correlation between mantle upwelling and maximum horizontal extension that is everywhere orthogonal to the axis of the rift system. This rift-related deformation, analogous to that predicted under the mid-Atlantic ridge (Fig. 7), continues under the southern Indian Ocean and extends to the Africa–Antarctica plate boundary. This rift-related sublithospheric deformation field is also orthogonal (with few exceptions, see Region (I) in Supplementary Fig. S8) to the anisotropy inferred by local seismic studies of shear wave splitting (Gashawbeza et al., 2004; Kendall et al., 2005) which instead shows a pattern of anisotropy that is predominantly parallel to the rift axes. One explanation (Gashawbeza et al., 2004; Kendall et al., 2005) for this discrepancy is the impact of volcanic activity in the form of shallow rift-aligned magmatic dykes and eruptive segments. This 'shape preferred orientation' closely follows the dominant rift-aligned pattern of asthenospheric flow we predict below the northern half of the EARS (Fig. 7).

A remarkable aspect of the EARS is the strong sub-horizontal asthenospheric flow field that sweeps under the entire north-south extent of the rift system, from southeast Africa to the Red Sea (see Fig. 5a). The interaction of this strong horizontal flow with local asthenospheric upwellings (Fig. S8) results in a deformation pattern akin to that analysed by Kaminski and Ribe (2002) in their plume-ridge interaction model. In this model (see Fig. **7** in Kaminski and Ribe 2002) the predicted LPO above the centralaxis of the upwelling plume is almost co-linear with the orientation of the regional ridge-flow pattern, and the local flow directions in the vicinity of the plume show a characteristic angular deviation pattern relative to the LPO (i.e. the fast *a*-axes). This fundamental character of the plume-ridge flow model also appears in the detailed flow-anisotropy correlations presented in Fig. S8.

7. Concluding comments

It has long been assumed that large-scale, deep-mantle dynamics under the African plate are dominated by the influence of a superplume located under southern Africa (Hager et al., 1985; Silver et al., 1988; Lithgow-Bertelloni and Silver, 1998; Behn et al., 2004). Recent progress in joint seismic–geodynamic mapping of the 3-D distribution of chemical heterogeneity in the mantle (Simmons et al., 2007, 2009) has allowed us to re-examine the mantle dynamic importance of this 'South African Superplume' (SASP) (Fig. 5a,b) relative to a second large-scale buoyant upwelling under western

Africa (Fig. 5d), that we have termed the 'West African Superplume' (WASP). We find that the negative chemical buoyancy inferred within the core of the SASP opposes its positive thermal buoyancy and thereby exerts a strong stabilising control on the mantle flow driven by this plume (Fig. 6). This chemical stabilisation has important consequences for the relative importance of the African plate motion generated by the SASP, which we conclude is comparable to that generated by the WASP (Supplementary Fig. S6). The distinction between the mantle upwellings associated with the SASP and WASP is especially evident when we remove the effect of the opposing chemical buoyancy in the SASP (Fig. 6d). These twosuperplumes evolve, as they ascend into the lower-viscosity upper mantle, into two separate groups of more focussed plumes: one under northern and western Africa, arising from the WASP and the other under central and eastern Africa, arising from the SASP(see Fig. 6a,b).

An important characteristic of the chemical heterogeneity in the SASP is its rather remarkable vertical extent (Fig. 5a,b), such that significant compositional buoyancy is inferred more than a 1000 km above the CMB. This distribution of chemical heterogeneity, in particular the tilted aspect of the SASP and the associated 'tendrils' or 'blobs' of chemically distinct mantle that appear to be shedding away from the main upwelling centre (as in Fig. 5b), is very similar to that found in recent laboratory experiments of thermochemical convection (Kumagai et al., 2008) that have been carried out with intermediate buoyancy ratios similar to those we infer for the SASP. Numerical and laboratory simulations of thermochemical convection have demonstrated how large-scale flow sweeps chemical heterogeneity at the base of the mantle into the centres of the upwelling regions (Tackley, 1998; Davaille, 1999; McNamara and Zhong, 2005). The amount of chemical heterogeneity that is entrained upwards is sensitive to the buoyancy ratio and for intermediate values (in the range 0.3–0.6 inferred here) the upwellings may develop complex time-dependent morphologies marked by rising and sinking motions (e.g. Davaille, 1999, Kumagai et al., 2008). These fluid-mechanical experiments suggest that the unique compositional heterogeneity within the SASP will imply a thermal, chemical and dynamical evolution which is distinct from that of the WASP whose dynamics is inferred to be dominated by thermal buoyancy.

A longstanding challenge we have attempted to address in this study is the development of a fully self-consistent global model of mantle convection that incorporates a wide-range of geodynamic, seismological and mineral physical constraints on mantle buoyancy and viscosity structure. We have shown that such a model can provide a successful reconciliation of mantle density anomalies, containing both thermal and chemical origins, with a wide array of convection-related surface data on the African plate, including plate motions, dynamic topography and gravity anomalies. This reconciliation is an essential prerequisite to our current effort to provide realistic predictions of the buoyancy-driven mantle flow at all depths under the African plate. In this regard, we refer to Burke's (1996) wide-ranging discursive review of African dynamics over the past 30 million years, in which he argued: "*Geophysics, including mantle tomography, satellite altimetry, seismic, gravity and magnetic studies, will all helpto clarify the structure of the African Plate and of the mantle beneath it.*" He further noted that, "*... an integrated approach to problem solving for the understanding of the past 30 Ma history of the African Plate is essential.*" The results we have obtained here should go some way to satisfying these objectives and they will serve as a basis for further studies of mantle convection dynamics under Africa, such as the recent effort to reconstruct the late Cenozoic evolution of African surface topography due to mantle convection (Moucha et al., 2009).

Acknowledgements

We are grateful for the very helpful and constructive review comments provided by Andy Nyblade and Anne Davaille. Postdoctoral support for RM was provided by the Canadian Institute for Advanced Research (CIFAR). AMF and JXM acknowledge funding from CIFAR and NSERC. AMF also thanks the Canada Research Chair program for the support. Work performed by NAS is under the auspices of the US Department of Energy under contract DE-AC52-07NA27344. SPG acknowledges NSF grant EAR0309189.

Appendix A. Supplementary data

Supplementary data associated with this article can be found, in the online version, at doi:10.1016/j.epsl.2010.03.017.

References

Allegre, C.J., Dupré, B., Lambret, B., Richard, P., 1981. The subcontinental versus suboceanic debate, 1 Lead-neodymium-strontium isotopes in primary alkali basalts from a shield area the Ahaggar volcanic suite. Earth Planet. Sci. Lett. 52, 85–92.
Barruol, G., Ben Ismail, W., 2001. Upper mantle anisotropy beneath the African IRIS and Geoscope stations. Geophys. J. Int. 146, 549–561.
Bastow, I.D., Nyblade, A.A., Stuart, G.W., Rooney, T.O., Benoit, M.H., 2008. Upper mantle seismic structure beneath the Ethiopian hot spot: rifting at the edge of the African low-velocity anomaly. Geochem. Geophys. Geosyst. 9, Q12022. doi:10.1029/2008GC002107.
Behn, M.D., Conrad, C.P., Silver, P.G., 2004. Detection of upper mantle flow associated with the African Superplume. Earth Planet. Sci. Lett. 224, 259–274.
Bunge, H.P., Richards, M.A., Baumgardner, J.R., 2002. Mantle-circulation models with sequential data assimilation: inferring present-day mantle structures from plate-motion histories. Phil. Trans. R. Soc. Lond. A 360, 2545–2567.
Burke, K., 1996. The African plate. S. Afr. J. Geol. 99, 341–410.
Conrad, C.P., Gurnis, M., 2003. Seismic tomography, surface uplift, and the breakup of Gondwanaland: integrating mantle convection backwards in time. Geochem. Geophys. Geosyst. 3, 1031. doi:10.1029/2001GC000299.
Crough, S.T., 1981. Free-air gravity over the Hoggar massif, northwest Africa: evidence for alteration of the lithosphere. Tectonophysics 77, 189–202.
Daradich, A., Mitrovica, J.X., Pysklywec, R.N., Willett, S.D., Forte, A.M., 2003. Mantle flow, dynamic topography, and rift-flank uplift of Arabia. Geology 31 (10), 901–904.
Davaille, A., 1999. Simultaneous generation of hotspots and superswells by convection in a heterogeneous planetary mantle. Nature 402, 756–760.
Davaille, A., Stutzmann, E., Silveira, G., Besse, J., Courtillot, V., 2005. Convective patterns under the Indo-Atlantic "box". Earth Planet. Sci. Lett. 239, 233–252.
Dziewonski, A.M., Anderson, D.L., 1981. Preliminary reference Earth model. Phys. Earth Planet. Inter. 25, 297–356.
Ebinger, C.J., Sleep, N.H., 1998. Cenozoic magmatism throughout east Africa resulting from impact of a single plume. Nature 395, 788–791.
Fishwick, S., White, N., Al-Hajri, Y., 2007. Small scale heterogeneity in the uppermost mantle and the dynamic topography on the west coast of Africa. Eos Trans. AGU 88 (52) Fall Meet. Suppl., Abstract S11B-0553.
Forte, A.M., 2007. Constraints on seismic models from other disciplines — implications for mantle dynamics and composition. In: Dziewonski, A.M., Romanowicz, B. (Eds.), Treatise of Geophysics, 1. Elsevier, Amsterdam, pp. 805–858.
Forte, A.M., 2000. Seismic–geodynamic constraints on mantle flow: implications for layered convection, mantle viscosity, and seismic anisotropy in the deep mantle. Earth's Deep Interior: Mineral Physics from the Atomic to the Global Scale: In: Karato, S.–.I., et al. (Ed.), AGU Geophys. Monogr. Ser., 117, pp. 3–36. Washington, DC.
Forte, A.M., Peltier, W.R., 1991. Viscous flow models of global geophysical observables 1. Forward problems. J. Geophys. Res. 96, 20131–20159.
Forte, A.M., Perry, H.K.C., 2000. Geodynamic evidence for a chemically depleted continental tectosphere. Science 290, 1940–1944.
Forte, A.M., Mitrovica, J.X., 2001. Deep-mantle high-viscosity flow and thermochemical structure inferred from seismic and geodynamic data. Nature 410, 1049–1056.
Forte, A.M., Woodward, R.L., Dziewonski, A.M., 1994. Joint inversions of seismic and geodynamic data for models of three-dimensional mantle heterogeneity. J. Geophys. Res. 99, 21857–21877.
Forte, A.M., Mitrovica, J.X., Espesset, A., 2002. Geodynamic and seismic constraints on the thermochemical structure and dynamics of convection in the deep mantle. Philos. Trans. R. Soc. London A 360, 2521–2543.
Gaboret, C., Forte, A.M., Montagner, J.P., 2003. The unique dynamics of the Pacific Hemisphere mantle and its signature on seismic anisotropy. Earth Planet. Sci. Lett. 208, 219–233.
Gashawbeza, E.M., Klemperer, S.L., Nyblade, A.A., Walker, K.T., Keranen, K.M., 2004. Shear-wave Splitting in Ethiopia: Precambrian Mantle Anisotropy Locally Modified by Neogene rifting 31, L18602. doi:10.1029/2004GL020471.
Grand, S.P., 2002. Mantle shear-wave tomography and the fate of subducted slabs. Philos. Trans. R. Soc. London A360, 2475–2491.
Gripp, A.E., Gordon, R.G., 2002. Young tracks of hotspots and current plate velocities. Geophys. J. Int. 150, 321–361.
Gurnis, M., Mitrovica, J.X., Ritsema, J., van Heijst, H.J., 2000. Constraining mantle density structure using geological evidence of surface uplift rates: the case of the African superplume. Geochem. Geophys. Geosyst. 3, 1 Paper number 1999GC000035.
Hadiouche, O., Jobert, N., Montagner, J.P., 1989. Anisotropy of the African continent inferred from surface waves. Phys. Earth Planet. Inter. 58, 61–81.
Hager, B.H., Clayton, R.W., Richards, M.A., Comer, R.P., Dziewonski, A.M., 1985. Lower mantle heterogeneity, dynamic topography and the geoid. Nature 313, 541–545.

Hammond, J.O.S., Kendall, J.-M., Rumpker, G., Wookey, J., Teanby, N., Joseph, P., Ryberg, T., Stuart, G., 2005. Upper mantle anisotropy beneath the Seychelles microcontinent. J. Geophys. Res. 110 (B11401). doi:10.1029/2005JB003757.
Hansen, S., Schwartz, S., Al-Amri, A., Rodgers, A., 2006. Combined plate motion and density-driven flow in the asthenosphere beneath Saudi Arabia: evidence from shear-wave splitting and seismic anisotropy. Geology 34, 869–872.
Hartley, R.W., Allen, P.A., 1994. Interior cratonic basins of Africa: relation to continental break-up and role of mantle convection. Basin Res. 6, 95–113.
Hess, H.H., 1964. Seismic anisotropy of the uppermost mantle under oceans. Nature 203, 629–631.
Kaminski, E., Ribe, N.M., 2002. Timescales for the evolution of seismic anisotropy in mantle flow. Geochem. Geophys. Geosyst 3 (3(8). doi:10.1029/2001GC000222.
Karato, S.-I., Jung, H., Katayama, I., Skemer, P., 2008. Geodynamic significance of seismic anisotropy of the upper mantle: new insights from laboratory studies. Annu. Rev. Earth Planet. Sci. 36, 59–95. doi:10.1146/annurev.earth.36.031207.124120.
Kendall, J.M., Stuart, G.W., Ebinger, C.J., Bastow, I.D., Keir, D., 2005. Magma-assisted rifting in Ethiopia. Nature 433, 146–148.
King, S.D., Ritsema, J., 2000. African hot spot volcanism: small-scale convection in the upper mantle beneath cratons. Science 290, 1137–1140.
Kumagai, I., Davaille, A., Kurita, K., Stutzmann, E., 2008. Mantle plumes: thin, fat, successful, or failing? Constraints to explain hot spot volcanism through time and space. Geophys. Res. Lett. 35, L16301. doi:10.1029/2008GL035079.
Lemoine, F., Pavlis, N., Kenyon, S., Rapp, R., Pavlis, E., Chao, B., 1998. New high-resolution model developed for Earth's gravitational field. Eos Trans. AGU 79 (9), 113.
Lithgow-Bertelloni, C., Silver, P.G., 1998. Dynamic topography, plate driving forces and the African superswell. Nature 395, 269–272.
McKenzie, D.P., 1979. Finite deformation during fluid flow. Geophys. J. R. Astron. Soc. 58, 689–715.
McNamara, A.K., Zhong, S., 2005. Thermochemical structures beneath Africa and the Pacific Ocean. Nature 437, 1136–1139.
Mitrovica, J.X., 1996. Haskell [1935] revisited. J. Geophys. Res. 101, 555–569.
Mitrovica, J.X., Forte, A.M., 2004. A new inference of mantle viscosity based upon joint inversion of convection and glacial isostatic adjustment data. Earth Planet. Sci. Lett. 225, 177–189.
Moucha, R., Forte, A.M., Rowley, D.B., Braun, J., Mitrovica, J.X., Simmons, N.A., Grand, S.P., 2009. Reconstructing African topography over the past 30 Myrs with high-resolution tomography-based convection modelling. Eos Trans. AGU 90 (52) Fall Meet. Suppl., Abstract DI32A-02.
Moucha, R., Forte, A.M., Mitrovica, J.X., Daradich, A., 2007. Lateral variations in mantle rheology: implications for convection related surface observables and inferred viscosity models. Geophys. J. Int. 169, 113–135.
Ni, S.D., Tan, E., Gurnis, M., Helmberger, D.V., 2002. Sharp sides to the African superplume. Science 296, 1850–1852.
Ni, S.D., Helmberger, D.V., Tromp, T., 2005. Three-dimensional structure of the African superplume from waveform modeling. Geophys. J. Int. 161, 283–294.
Nyblade, A.A., Robinson, S.W., 1994. The African superswell. Geophys. Res. Lett. 21, 765–768.
Poirier, J.-P., 1985. Creep of Crystals. Cambridge University Press, Cambridge, UK, p. 274.
Priestley, K., McKenzie, D., Debayle, E., 2006. The state of the upper mantle beneath southern Africa. Tectono Physics 416, 101–112.
Quéré, S., Forte, A.M., 2006. Influence of past and present-day plate motions on spherical models of mantle convection: implications for mantle plumes and hotspots. Geophys. J. Int. 165, 1041–1057.
Quéré, S., Rowley, D.B., Forte, A.M., Moucha, R., 2007. No-Net-Rotation and Indo-Atlantic hotspot reference frames: towards a new view of tectonic plate motions and Earth dynamics. Eos Trans. AGU 88 (52) Fall Meet. Suppl., Abstract U34A-03.
Ribe, N.M., 1992. On the relation between seismic anisotropy and finite strain. J. Geophys. Res. 97 (B6), 8737–8747.
Richards, M.A., Hager, B.H., 1984. Geoid anomalies in a dynamic Earth. J. Geophys. Res. 89, 5987–6002.
Ritsema, J., van Heijst, H.J., Woodhouse, J.H., 1999. Complex shear velocity structure imaged beneath Africa and Iceland. Science 286, 1925–1928.
Sahagian, D.L., 1993. Structural evolution of African basins: stratigraphic synthesis. Basin Res. 5, 41–54.
Sebai, A., Stutzmann, E., Montagner, J.P., Sicilia, D., Beucler, E., 2006. Anisotropic structure of the African upper mantle from Rayleigh and Love wave tomography. Phys. Earth Planet. Inter. 155, 48–62.
Silver, P.G., 1996. Seismic anisotropy beneath the continents: probing the depths of geology. Annu. Rev. Earth Planet. Sci. 24, 385–432.
Silver, P.G., Carlson, R.W., Olson, P., 1988. Deep slabs, geochemical heterogeneity, and the large-scale structure of mantle convection: investigation of an enduring paradox. Annu. Rev. Earth Planet. Sci. 16, 477–541.
Silver, P.G., Gao, S.S., Liu, K.H., Kaapvaal Seismic Group, 2001. Mantle deformation beneath southern Africa. Geophys. Res. Lett. 28, 2493–2496.
Simmons, N.A. Mantle heterogeneity and flow from seismic and geodynamic constraints. Doctoral Dissertation, University of Texas at Austin, pp. 262 (2007).
Simmons, N.A., Forte, A.M., Grand, S.P., 2007. Thermochemical structure and dynamics of the African superplume. Geophys. Res. Lett. 34, L02301. doi:10.1029/2006GL028009.
Simmons, N.A., Forte, A.M., Grand, S.P., 2009. Joint seismic, geodynamic and mineral physical constraints on three-dimensional mantle heterogeneity: implications for the relative importance of thermal versus compositional heterogeneity. Geophys. J. Int. 17 (3), 1284–1304.
Tackley, P.J., 1998. Three-dimensional simulations of mantle convection with a thermochemical CMB boundary layer: D"? In: Gurnis, M., Wysession, M.E., Knittle, E., Buffett, B.A. (Eds.), The Core–Mantle Boundary Region, 28. AGU, Washington, DC, pp. 231–253.
Thorpe, R.S., Smith, K., 1974. Distribution of Cenozoic volcanism in Africa. Earth Planet. Sci. Lett. 22, 91–95.
Vinnik, L.P., Green, R.W.E., Nicolaysen, L.O., 1995. Recent deformations of the deep continental root beneath southern Africa. Nature 375, 50–52.
Walker, K.T., Nyblade, A.A., Klemperer, S.L., Bokelmann, G.H.R., Owens, T.J., 2004. On the relationship between extension and anisotropy: Constraints from shear wave splitting across the East African Plateau. J. Geophys. Res. 109 (B08302). doi:10.1029/2003JB002866.
Zhang, S., Karato, S.-I., 1995. Lattice preferred orientation of olivine aggregates deformed in simple shear. Nature 375, 774–777.